European Conference on Optical Communication (ECOC) 2022 © Optica Publishing Group 2022

Mid-IR Plasmonics for Monolithic Photonic Integrated Circuits

Borislav Hinkov[(1)], Florian Pilat[(1)], Mauro David[(1)], Andreas Schwaighofer[(2)], Patricia L. Souza[(1,3)], Laurin Lux[(2)], Bettina Baumgartner[(2,4)], Daniela Ristanic[(1)], Benedikt Schwarz[(1)], Hermann Detz[(1,5)], Aaron M. Andrews[(1)], Bernhard Lendl[(2)] and Gottfried Strasser[(1)]

[(1)] Institute of Solid State Electronics & Centre for Micro- & Nanostructures, TU Wien, Vienna, Austria, borislav.hinkov@tuwien.ac.at
[(2)] Institute of Chemical Technologies and Analytics, TU Wien, Vienna, Austria
[(3)] LabSem-CETUC, Pontifícia Universidade Católica do Rio de Janeiro, Rio de Janeiro, Brazil
[(4)] Debye Institute for Nanomaterials Science, Utrecht University, Utrecht, Netherlands
[(5)] CEITEC, Brno University of Technology, Brno, Czech Republic

Abstract *We present a monolithic mid-infrared lab-on-a-chip for sensitive and selective real-time spectroscopy of liquids. Beyond state-of-the-art operation of our fingertip-sized sensor devices is demonstrated by in-situ reaction monitoring experiments of thermally-induced protein-conformational changes and by dynamical residual-water analysis in a solvent.* *©2022 The Author(s)*

Introduction

Sensors are an important element of our daily life, addressing e.g. medical, environmental, security or telecommunication applications [1-4]. Mid-infrared (mid-IR) spectroscopy is a sensitive and selective technique for assessing the fundamental fingerprint absorption of gaseous or liquid molecules and thus realize high-performance optical sensors.

However, in particular mid-IR liquid-phase spectroscopy is still limited to bulky detection systems, often requiring time-consuming offline analytics [5-6]. Therefore, the realization of highly-sensitive and -selective sensors for real-time monitoring of dynamic processes in liquids in analytical chemistry and bio-medical applications is still hampered by the lack of suitable concepts that can be matched with existing cutting-edge technology.

In this paper, we address the challenging task and present a solution by demonstrating a next generation mid-IR chemical sensor that is exploited in monitoring dynamical analytical processes in real time. Based on pioneering quantum cascade (QC) technology, that is combined with monolithic integration strategies exploiting novel mid-IR plasmonic concepts, we realize a fingertip-sized photonic integrated circuit (PIC) in the form of a robust lab-on-a-chip device. Based on finite-element simulations, that confirm its suitable operation in liquid environment, it is designed to address time-resolved sensor operation by real-time monitoring of two different types of experiments: thermally-induced protein-conformational changes and residual water analysis in a solvent. Both settings display relevant situations in analytical chemistry, requiring real-time analysis.

Monolithic PIC geometry

Our on-chip sensor combines a spectrally optimized QC laser (QCL) and QC detector (QCD) with similar emission and detection wavelength [7] into a single chip. Such a device is also referred to as QCLD. As displayed in Fig. 1, both devices are realized in a ridge geometry, separated by a gap on the order of 10s to 100s of micrometres. For suitable mode-guiding between laser and detector, we use novel mid-IR plasmonic waveguides, based on dielectric-loaded surface plasmon polaritons (DLSPPs) [8,9].

They consist of a SiN-slab placed on top of a gold plasmonic layer. The dielectric material on top is responsible for much better confining the plasmonic mode as compared to a bare gold-based plasmonic waveguide. Their remarkable advantages include the before mentioned highly efficient mode propagation with propagation lengths on the order of 100s of micrometres to even millimetres along the chips surface,

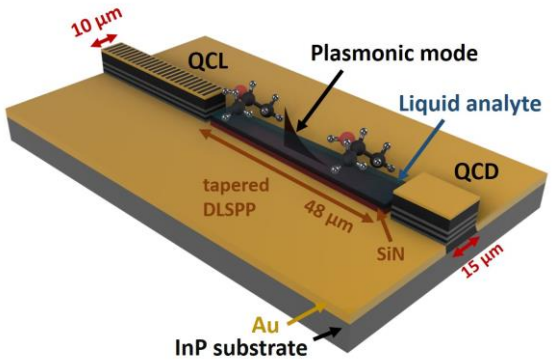

Fig. 1: Sketched QCLD-based sensor including labeling of its relevant layers. For clarity, the liquid sample is only displayed on top of the plasmonic interaction section.

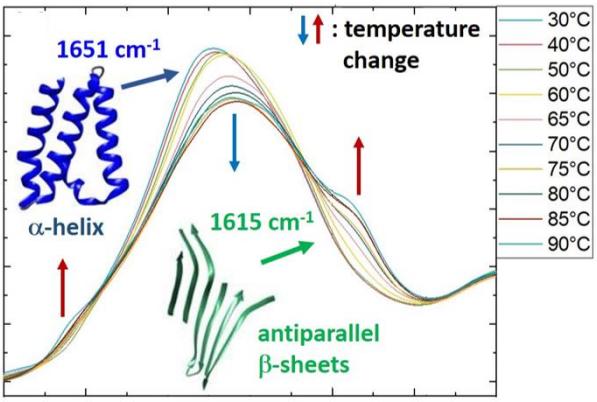

Fig. 2: Thermally induced spectral changes of the BSA protein, when heated from 30°C to 90°C.

together with simultaneously guiding the mode mainly within the surrounding medium (typically >95% of the mode are guided outside).

The particular device dimensions are given in Fig. 1, while the device active region (AR) design addressing the 1600 – 1700 cm^{-1} spectral range can be found in [8]. This range is known as the amide I band and is suitable for addressing various proteins and solvents.

Liquid analyte and background matrix

For calibrating the sensor in a first set of experiments, we selected to analyse the dynamically changing water content in an isopropyl alcohol (IPA) matrix. In quality control of solvents as part of chemical processes, e.g. in drug production, residual water content is one parameter for the quality of solvents, often defining the optimum productivity and performance of the final product.

We investigate H_2O in IPA matrix at around 1650 cm^{-1}, where water shows high and IPA low absorption. We directly submerged the whole sensor chip into the beaker with the sample for demonstrating its capabilities in *in-situ* real-time monitoring. By continuously increasing the water concentration in the sample, we measured the remaining optical signal on the on-chip QCD.

In the second set of experiments, we monitor the thermal denaturation process of the model protein bovine serum albumin (BSA) in a D_2O matrix. BSA irreversibly unfolds from an α-helix structure at around room temperature to antiparallel β-sheets typically between 50°C – 70°C and above, depending on the BSA concentration (see Fig. 2 for temperature-dependent BSA-spectra). Due to the strong water absorptions in the protein amide I region, we substitute it with its counterpart D_2O. It has much lower absorptions in this range, thus allowing us to fully analyse our sensor in its low concentration rage, distinguish accurately its limit of detection (LOD) and demonstrate its long propagation length of the plasmonic mode way beyond the typically used 10-25 µm [10,11] of existing mid-IR spectroscopic systems. We want to further stress, that the actual denaturation process as displayed by its spectral changes when heating the sample from 30°C to 90°C in Fig. 2, is very similar in D_2O and H_2O, with the main difference of a changing transition temperature [12]. Thus, measuring in heavy water comes close to native protein conditions.

We perform two experiments: a calibration line measurement by submerging the whole chip into the BSA+D_2O sample with varying analyte concentrations and the thermal denaturation experiments, using a custom-made 60-µl cell.

Experimental Configurations

In the direct submersion geometry, the experimental setup consists of a beaker, initially only containing the low absorbing liquid matrix (i.e. either the IPA for the water analysis or heavy water, when performing the experiments with BSA). Using a multi-channel peristaltic pump, we continuously pump the analyte, i.e. water or BSA, into the beaker with the sensor under operation, and monitor its detector signal.

When using the 60-µl liquid flow cell together with the on-chip sensor, we start by pumping the pure analyte through the cell, while overtime either adding increasing amounts of water (solve analysis) or starting to pump the BSA-D_2O stock solution at a fixed concentration through the cell and continuously increasing its temperature from 30°C to 90°C. The measurement of the BSA unfolding process is conducted at about 21°C, after quickly cooling down the microliter-scale liquid back to the measurement temperature within a few seconds only.

For all experiments in beakers, stirring magnets are used, for a homogeneous distribution of the analyte in the background matrix.

Dynamical Analysis of Solvent Quality

The measurements of the residual water content in IPA are performed by adding little amounts of deionized (DI-) water at a rate of ~200 µl/min to the beaker filled with IPA into which our QCLD sensor is submerged. The increasing absorption from the added water is monitored using the on-

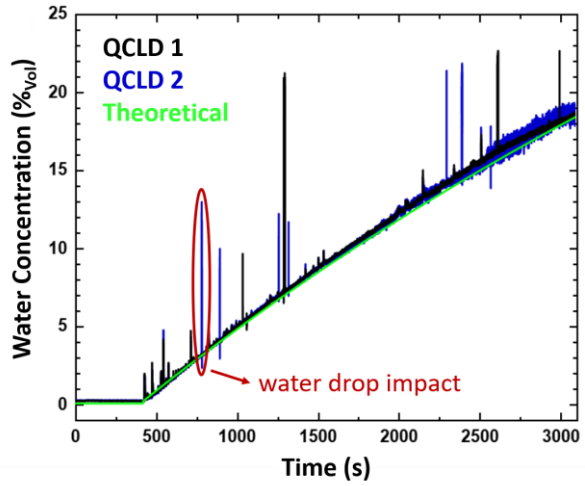

Fig. 3: Water concentration curve as function of time when submerging the QCLD in-situ into the sample beaker. The blue and black line correspond to two QCLDs at 1650 cm^{-1} in comparison to the theoretical water curve in green. The observed "spikes" correspond to the impact of the water droplets into the beaker with the QCLD and the H_2O-IPA mixture.

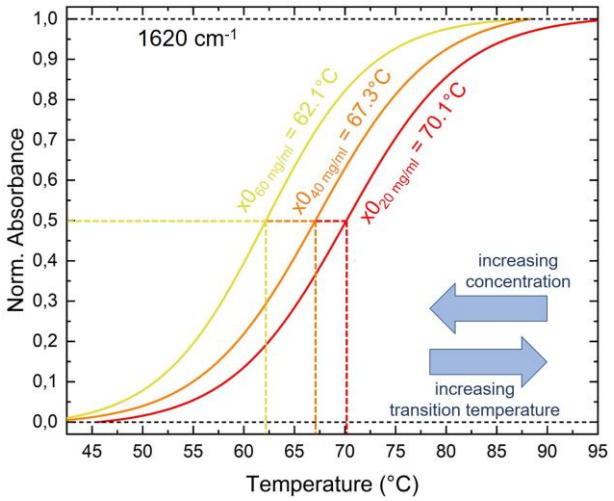

Fig. 4: Normalized concentration-dependent denaturation curves at 1620 cm^{-1}, when increasing the temperature up to 90°C. With increasing concentration, we observe the typical decreasing transition temperature [av].

chip QCD and translates into the actual water concentration in the beaker. Applying an additional temperature correction by using an on-chip temperature probe (basically monitoring the change in resistance of a neighbouring QCL device on the same chip), helps to further improve the measured signal. Figure 3 shows the results for two QCLD sensors from the same chip, both addressing the wavelength-range around 1650 cm^{-1} and in comparison to the theoretical curve. The good overlap between theory and measurement holds up to about 19% of water and we obtain a limit of detection of about 150 ppm. This is comparable to state-of-the-art offline chemical analysis techniques like Karl-Fischer titration as probably the most prominent among them [13].

Thermal Denaturation of BSA in real time [14,15]

Next, we characterized a similar sensor but addressing 1620 cm^{-1} for its capabilities in the dynamical monitoring of the BSA denaturation process, when using a 60-µl liquid flow cell together with the QCLD chip. As shown in Fig. 4, we measure the typical s-shaped denaturation curves, known from previous experiments and also other proteins. Moreover, we can additionally confirm the trend of decreasing transition temperature with increasing BSA concentration in the D_2O matrix. This is another important confirmation of the validity of the results. From additional submersion measurements we obtain the calibration line of our sensor for BSA in D_2O. We can further extract important figures-of-merit which go beyond state-of-the-art (e.g. LOD). They include a 55-times higher absorbance value, LOD of 75 ppm and a coverage of more than 3 orders of BSA-concentrations between 0.0075% and 9.23%.

Those results are remarkable, since our sensor is also much more compact and can be used for real-time measurements in *in-situ* configuration.

Conclusions

In conclusion, we showed a novel mid-IR PIC devise based on mid-IR plasmonic concepts and QC technology, suitable for pushing the boundary in analytical chemistry of liquids much beyond the current state-of-the-art. By enabling dynamic reaction monitoring experiments in real-time, it unlocks a previously inaccessible type of measurements.

Outlook

After achieving our fundamental results, we will further extend the mid-IR plasmonic platform towards on-chip heterodyne detectors for mid-IR telecommunication applications. Exploiting similar concepts as presented above, they allow on-chip beam guiding and directing on the millimetre-scale, enabling monolithic heterodyne detectors. They facilitate the measurement of low optical signal through beating with an on-chip local oscillator, which are typical from optical free-space telecommunication experiments.

Acknowledgments

This work received funding from the EU Horizon 2020 Framework Program (project No. 828893, 780240) and the Austrian Science Fund FWF (M2485-N34).

References

[1] K. V. Sreekanth, Y. Alapan, M. Elkabbash, E. Ilker, M. Hinczewski, U. A. Gurkan, A. De Luca, and G. Strangi, "Extreme sensitivity biosensing platform based on hyperbolic metamaterials," *Nature Materials*, vol. 15, pp. 621-627, 2016, DOI: 10.1038/nmat4609.

[2] F. Schreiber, P. Wunderlin, K. M. Udert, and G. F. Wells, "Nitric oxide and nitrous oxide turnover in natural and engineered microbial communitites", *Frontiers in Microbiolgy*, vol. 3, pp. 1–24, 2012, DOI: 10.3389/fmicb.2012.00372.

[3] B. Hinkov, F. Fuchs, Q. K. Yang, J. M. Kaster, W. Bronner, R. Aidam, K. Köhler, and J. Wagner, "Time-resolved spectral characteristics of external-cavity quantum cascade lasers and their application to stand-off detection of explosives", *Applied Physics B*, vol. 100, pp. 253–260, 2010, DOI: 10.1007/s00340-009-3863-7.

[4] H. Dely, T. Bonazzi, O. Spitz, E. Rodriguez, D. Gacemi, Y. Todorov, K. Pantzas, G. Beaudoin, I. Sagnes, L. Li, A. G. Davis, E. H. Linfield, F. Grillot, A. Vasanelli, and C. Sirtori, "10 Gbit s^{-1} Free Space Data Transmission at 9 µm Wavelength With Unipolar Quantum Optoelectronics", *Laser and Photonics Reviews*, vol. 16, no. 2, pp. 1–7, 2022, DOI: 10.1002/lpor.202270006.

[5] J. Haas and B. Mizaikoff, "Advances in Mid-Infrared Spectroscopy for Chemical Analysis", *Annual Review of Analytical Chemistry*, vol. 9, pp. 45–68, 2016, DOI: 10.1146/annurev-anchem-071015-041507.

[6] A. Dabrowska, M. David, S. Freitag, A. M. Andrews, G. Strasser, B. Hinkov, A. Schwaighofer, and B. Lendl, "Broadband laser-based mid-infrared spectroscopy employing a quantum cascade detector for milk protein analysis", *Sensors and Actuators B*, vol. 350, 130873, 2022, DOI: 10.1016/j.snb.2021.130873.

[7] B. Schwarz, C. A. Wang, L. Missagia, T. Mansuripur, P. Chevalier, M. K. Connors, D. McNulty, J. Cederberg, G. Strasser, and F. Capasso, "Watt-Level Continuous-Wave Emission from a Bifunctional Quantum Cascade Laser/Detector", *ACS Photonics*, vol. 4, no. 5, pp. 1225–1231, 2017, DOI: 10.1021/acsphotonics.7b00133.

[8] B. Schwarz, P. Reininger, D. Ristanic, H. Detz, A. M. Andrews, W. Schrenk, and G. Strasser, "Monolithically integrated mid-infrared lab-on-a-chip using plasmonics and quantum cascade structures", *Nature Communications*, vol. 5, pp. 4085, 2014, DOI: 10.1038/ncomms5085.

[9] M. David, A. Dabrowska, M. Sistani, I. C. Doganlar, E. Hinkelmann, H. Detz, W. M. Weber, B. Lendl, G. Strasser, and B. Hinkov, "Octave-spanning low-loss mid-IR waveguides based on semiconductor-loaded plasmonics", *Optics Express*, vol. 29, no. 26, pp. 43567–43579 , 2021, DOI: 10.1364/OE.443966 Journal.

[10] H. Fabian and W. Mäntele, "Infrared Spectroscopy of Proteins", *Handbook of Vibrational Spectroscopy*, Hoboken, NJ: John Wiley & Sons, Inc., 2006, DOI: 10.1002/0470027320.s8201.

[11] A. Schwaighofer, C. K. Akhgar, and B. Lendl, "Broadband laser-based mid-IR spectroscopy for analysis of proteins and monitoring of enzyme activitiy", *Spectrochimica Acta A*, vol. 253, pp. 119563, 2021, DOI: 10.1016/j.saa.2021.119563.

[12] X. Zhou, Z. He, and H. Huang, "Secondary structure transitions of Bovine serum albumin induced by temperature variation", *Vibrational Spectroscopy*, vol. 92, pp. 273–279, 2017, DOI: 10.1016/j.vibspec.2017.08.001.

[13] E. Scholz, "Karl Fischer Titration: Determination of Water", Berlin Heidelberg: Springer, 1984, DOI: 10.1007/978-3-642-69368-7.

[14] B. Hinkov, M. David, F. Pilat, L. Lux, P. Lustoza Souza, A. Schwaighofer, B. Schwarz, H. Detz, A. M. Andrews, B. Lendl, and G. Strasser, "Mid-IR plasmonics for next generation liquid sensing", *invited presentation at the 10th SciX conference (47th Federation of Analytical Chemistry & Spectroscopy Societies (FACSS)*, Providence (Rhode Island), USA, 26 Sept. – 01 Oct.,2021.

[15] B. Hinkov, F. Pilat, L. Lux, P. Lustoza Souza, M. David. A. Schwaighofer, D. Ristanic, B. Schwarz, H. Detz, A. M. Andrews, B. Lendl, and G. Strasser, "A mid-infrared lab-on-a-chip for dynamic reaction monitoring, *currently under review*, 02/2022.